(Received 12 August 2025, Accepted 30 September 2025, Scheduled 20 October 2025)

Reconfigurable Multilayer Graphene Antenna for Terahertz Sensing: Machine Learning-Based Frequency and Bandwidth Estimation

Hamza Ben Krid*, Aymen Hlali, and Hassen Zairi

Research Laboratory Smart Electricity and ICT, SEICT
National Engineering School of Carthage, University of Carthage, Tunis, Tunisia

ABSTRACT: This paper presents a reconfigurable multilayer graphene antenna for terahertz sensing, machine learning-based frequency, and bandwidth estimation. The antenna utilizes the tunable electromagnetic properties of graphene, enabling dynamic reconfiguration of the resonant frequency and bandwidth. By adjusting key physical parameters including chemical potential, relaxation time, and temperature, the antenna achieves frequency tuning from 1.542 THz to 1.562 THz, with an improved return loss reaching −30.8 dB and a bandwidth range from 91 GHz to 96 GHz. Furthermore, the resonance frequency and bandwidth are predicted using machine learning algorithms, including Random Forest and XGBoost, with results that closely match simulation data. These results highlight the potential of the proposed structure not only for adaptive communication systems but also for terahertz sensing platforms requiring frequency agility and environmental responsiveness.

1. INTRODUCTION

The rapid evolution of wireless communication systems is progressively steering technologies toward the terahertz (THz) frequency spectrum, particularly in the 1–2 THz range, which holds immense potential for next-generation high-speed data transmission, sensing, and high-resolution imaging [1, 2]. Within this frequency band, antennas play a pivotal role, serving as the primary interface for transmitting and receiving electromagnetic waves that carry information [3]. However, operating in the THz domain introduces critical design challenges for conventional antennas, particularly in terms of radiation efficiency, impedance bandwidth, and dynamic adaptability to varying application requirements [4, 5].

To overcome the inherent challenges of THz antenna design and fully harness the capabilities offered by this spectral window, current research is increasingly focused on the integration of advanced nanomaterials [6]. Among them, graphene has gained significant attention due to its tunable conductivity, high carrier mobility, and plasmonic behavior at terahertz frequencies [7]. These properties make it a strong candidate for enabling novel antenna architectures. In particular, embedding graphene within multilayer structures opens up new design pathways to achieve improved reconfigurability [8], compactness, and adaptability [9, 10], which are essential for high performance THz sensing and imaging systems [11, 12].

Recently, multilayer antenna designs have attracted considerable attention due to their ability to enhance key performance metrics [13]. In the terahertz frequency range, where traditional antenna solutions often face constraints, multilayer structures offer promising avenues to overcome challenges such as impedance matching, radiation efficiency, and beam steering [14, 15]. By carefully stacking layers with distinct electromagnetic characteristics, these antennas enable tailored responses to THz waves, facilitating precise control over radiation patterns and polarization states [4].

Central to this innovative approach is graphene, a two-dimensional carbon allotrope distinguished by exceptional electrical, thermal, and mechanical properties. Its notably high carrier mobility and electrically tunable conductivity offer new opportunities in antenna design [16, 17]. Moreover, graphene's ultra-wideband response extending into the terahertz range makes it particularly well-suited to overcoming the bandwidth limitations typically encountered by conventional antennas at these frequencies [18].

The development of hybrid structures that combine the advantages of diverse materials has driven significant progress across multiple disciplines [19]. In the realm of terahertz antennas, integrating graphene with conventional metals creates a synergistic platform that leverages the high electrical conductivity and mechanical stability of metals alongside the exceptional tunability of graphene. Such hybridization not only enhances the overall performance but also introduces new functionalities that are difficult to achieve with a single material. Specifically, incorporating graphene within a multilayer antenna design allows for precise modulation of its surface conductivity through external stimuli, such as chemical potential variation or applied gate voltage [20]. This capability enables dynamic tuning of the antenna's resonance frequency, band-

* Corresponding author: Hamza Ben Krid (hamza.benkrid@enicar.u-carthage.tn).

width, and radiation properties, making it well-suited for reconfigurable THz systems and adaptive sensing platforms [7]. The proposed hybrid approach combines the tunable electronic properties of graphene with the high conductivity and mechanical robustness of metallic layers, offering enhanced adaptability. Through external biasing of the graphene layer, it becomes possible to precisely control the resonance frequency, bandwidth, and impedance matching. As a result, the antenna can be reconfigured in real time without physical alterations, minimizing downtime and improving operational efficiency. This is particularly beneficial for THz communication systems, where varying channel conditions demand rapid frequency agility. Additionally, the architecture supports multifunctional operation, including high-resolution imaging and accurate gas or biomolecular detection. Overall, the metal-graphene hybrid structure establishes a flexible and reliable platform that meets the performance demands of next-generation THz devices [21].

Recently, deep learning has shown strong potential in modeling complex THz systems by predicting device responses from design parameters such as chemical potential, relaxation time, and temperature. These models reduce reliance on full-wave simulations and enable real-time parameter sweeps. Once trained, they can rapidly identify optimal configurations for tunable and reconfigurable graphene-based devices. This physics-informed, data-driven approach accelerates design workflows for THz applications [22, 23]. Additionally, ensemble learning methods such as XGBoost and Random Forest have been effectively applied to estimate key parameters resonance frequency and bandwidth considering variations in chemical potential, temperature, and relaxation time. These data driven approaches offer efficient alternatives to traditional simulations, accelerating the design of reconfigurable THz components [24].

Although significant progress has been made on graphene-based antennas, most reported works remain confined to single-layer designs, with limited exploration of multilayer configurations such as Graphene, Al_2O_3 and SiO_2 that could enhance tunability and efficiency. The application of machine learning in this field is also relatively scarce, and existing studies often restrict their predictions to a single parameter, typically the resonance frequency. Moreover, the combined influence of chemical potential, relaxation time, and temperature on both resonance frequency and bandwidth has not been systematically addressed. At the same time, the potential of hybrid copper graphene architectures to provide stable radiation performance while enabling dynamic reconfigurability is still underexplored. To fill these gaps, this work proposes a multilayer reconfigurable antenna that integrates a copper patch with graphene layers, while employing ensemble learning models (Random Forest and XGBoost) to accurately predict both frequency and bandwidth. This approach not only offers an efficient and versatile platform for next generation terahertz communication and sensing applications, but also significantly reduces the computational cost by saving considerable simulation time.

The organization of this paper unfolds as follows. Section 2 outlines the presented antenna design. Section 3 is devoted to the modeling of graphene surface conductivity, while Section 4 provides a detailed comparison of the proposed structure using different 2D materials, followed by a discussion of the results obtained from the main multilayer antenna based on graphene and its reconfiguration using the chemical potential. Section 5 is dedicated to the prediction of the resonance frequency and bandwidth using machine learning techniques, where two algorithms, namely Random Forest and XGBoost are compared based on their ability to estimate the frequency and bandwidth response. Finally, the concluding section encapsulates the primary insights and conclusions derived from this study.

2. DESIGN OF THE PROPOSED ANTENNA

The proposed antenna is a reconfigurable multilayer structure integrating both graphene and copper. It is composed of a SiO_2 substrate with a relative permittivity of $\mu_r = 3.9$, followed by an Al_2O_3 substrate with $\mu_r = 9.9$. An atomically thin graphene layer (0.01 µm) is deposited on top of the Al_2O_3 substrate, serving as the active tunable element. Finally, a circular copper patch is placed above the graphene layer, acting as the main radiating element. In this hybrid configuration, the copper patch ensures stable radiation patterns, while the graphene layer enables dynamic reconfiguration of the antenna's resonance frequency and bandwidth by tuning its surface conductivity. This combination allows the structure to efficiently adapt to different operating conditions without compromising radiation stability. Figure 1 illustrates the schematic diagram of the proposed multilayer reconfigurable THz antenna.

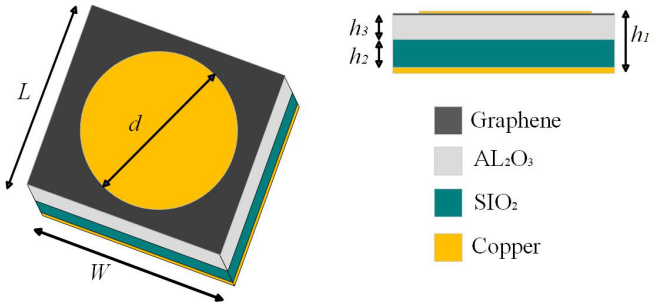

FIGURE 1. Schematic views of the proposed multilayer reconfigurable THz antenna in side view and top view.

The optimized structural dimensions of the proposed THz reconfigurable antenna are summarized in Table 1.

TABLE 1. Design parameters of the THz reconfigurable antenna.

Parameters	h_1	h_2	h_3	W	L	d
Values (µm)	40.15	20	20	80	80	40

3. MODELING OF GRAPHENE SURFACE CONDUCTIVITY

Graphene's surface conductivity, denoted by $\sigma(\omega)$, plays a fundamental role in its interaction with electromagnetic waves, especially in the terahertz frequency range. This complex quantity arises from two distinct quantum contributions: intraband and interband electronic transitions. The conductivity is highly

sensitive to the chemical potential μ_c), which can be externally modulated through gate voltage, electrostatic biasing, substrate engineering, or chemical doping. As μ_c varies, both the real and imaginary parts of $\sigma(\omega)$ experience significant changes, making graphene an excellent candidate for reconfigurable THz components [25, 26]. When graphene is considered as a two-dimensional conductive sheet, the total surface conductivity of graphene is typically expressed as [27, 28]:

$$\sigma(\omega) = \sigma_{\text{intra}}(\omega) + \sigma_{\text{inter}}(\omega) \tag{1}$$

In the THz frequency range, the intraband contribution usually dominates and can be formulated as:

$$\sigma_{\text{intra}}(\omega) = -j \frac{e^2 k_B T}{\pi \hbar^2 (\omega - j2\gamma)} \left[\frac{\mu_c}{k_B T} + 2 \ln \left(1 + e^{-\mu_c/(k_B T)} \right) \right] \tag{2}$$

In the low-temperature limit ($k_B T \ll \mu_c$), this can be further approximated by a Drude like model:

$$\sigma_{\text{Drude}}(\omega) = \frac{e^2 \mu_c}{\pi \hbar^2} \cdot \frac{1}{\gamma - j\omega} \tag{3}$$

While interband transitions are negligible at low THz frequencies, they are included here for completeness. The simplified expression reads:

$$\sigma_{\text{inter}}(\omega) = -j \frac{e^2}{4\pi\hbar} \left[\frac{2|\mu_c| - \hbar(\omega - j2\gamma)}{2|\mu_c| + \hbar(\omega - j2\gamma)} \right] \tag{4}$$

Since $\sigma(\omega)$ is a complex quantity, it corresponds to a surface impedance $Z_s(\omega)$, given by:

$$Z_s(\omega) = \frac{1}{\sigma(\omega)} = R_s + jX_s \tag{5}$$

where:

$$R_s = \Re \left(\frac{1}{\sigma(\omega)} \right) \tag{6}$$

$$X_s = \Im \left(\frac{1}{\sigma(\omega)} \right) \tag{7}$$

Here, R_s and X_s represent the surface resistance and reactance, respectively. These parameters are essential in full-wave electromagnetic solvers such as Computer Simulation Technology (CST) and High Frequency Structure Simulator (HFSS), where accurate material modeling is crucial. The physical constants and variables are defined as follows: μ_c is the chemical potential (eV), k_B the Boltzmann's constant, T the absolute temperature (K), $\gamma = 1/\tau$ the scattering rate (s^{-1}), $\hbar$ the reduced Planck constant, ω the angular frequency (rad/s), and e the elementary charge.

These relations highlight how the optical and electronic properties of graphene can be finely tuned to realize highly adaptive THz devices. Figure 2 illustrate the real and imaginary

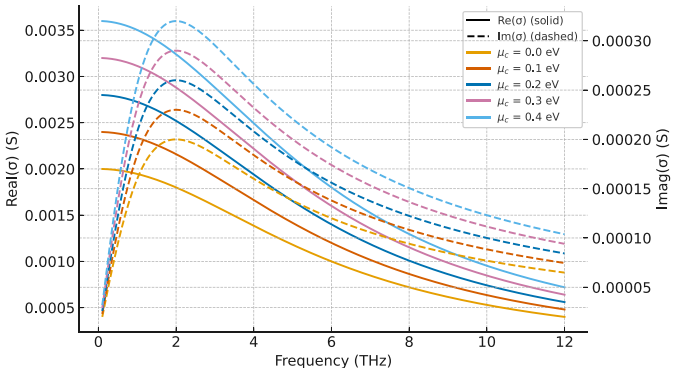

FIGURE 2. Refial and imaginary part of the graphene conductivity versus frequency for different chemical potential values.

parts of the graphene surface conductivity $\sigma(\omega)$ as a function of frequency for five different chemical potentials: 0 eV, 0.1 eV, 0.2 eV, 0.3 eV, and 0.4 eV. The simulations were carried out at a constant temperature of 300 K and a relaxation time of 0.1 ps. The results clearly demonstrate how tuning the chemical potential alters both components of the conductivity, enabling effective control of the electromagnetic response. The relationship between the applied gate voltage V_g and chemical potential μ_c is given by:

$$V_g = \frac{h\mu_c^2 e}{\nu_f^2 \varepsilon_0 \varepsilon_r h^2} \tag{8}$$

where ε_r is the substrate's relative permittivity, ε_0 the vacuum permittivity, h the substrate thickness, and ν_f the Fermi velocity in graphene.

Figure 3 illustrates the nonlinear relationship between the applied gate voltage and the chemical potential in graphene, highlighting the stronger electric fields required for higher chemical potentials. This electrostatic tunability is a cornerstone of reconfigurable THz graphene-based devices.

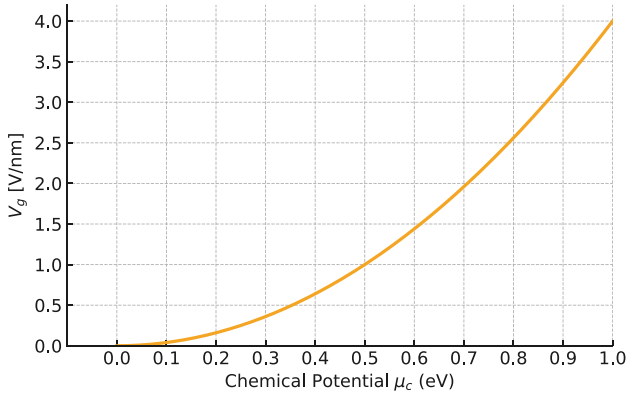

FIGURE 3. Voltage applied to graphene.

4. EVALUATION OF 2D MATERIAL-BASED ANTENNA STRUCTURES AND GRAPHENE RECONFIGURABILITY

4.1. Comparative Analysis of 2D Materials

To better evaluate the performance of the proposed structure, a comparative analysis was conducted among the proposed an-

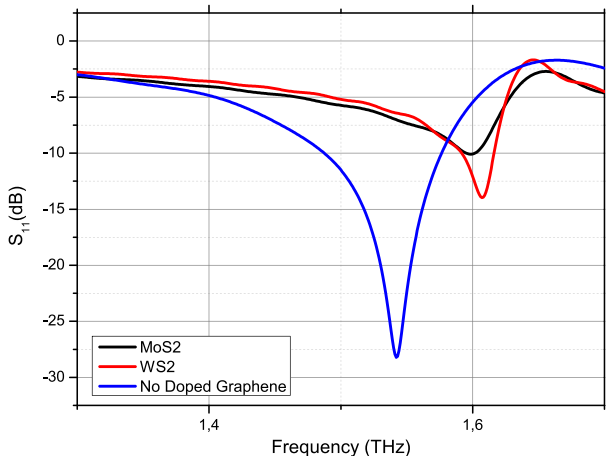

FIGURE 4. Reflection coefficient S_{11} curves for no-doped graphene, WS_2, and $MoSe_2$ based antennas in the THz frequency range.

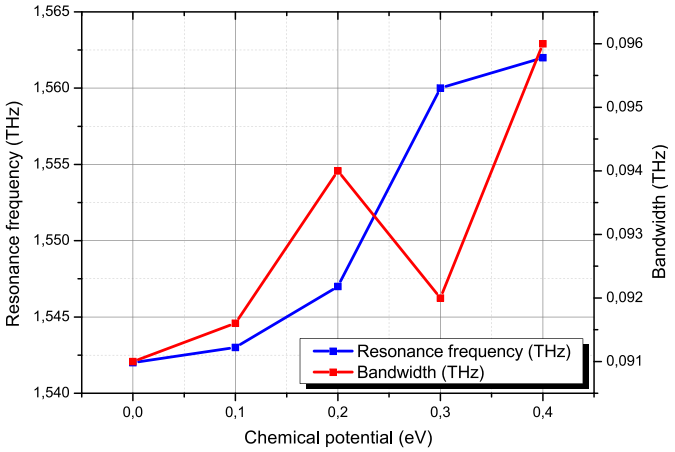

FIGURE 6. Resonant frequency and bandwidth versus different values of chemical potential.

tenna using CST Microwave Studio, no-doped graphene, WS_2, and $MoSe_2$, which are commonly used two-dimensional (2D) materials in the THz region. All simulations were performed under identical conditions. The performance of the antennas was assessed using a key parameter, namely the reflection coefficient (S_{11}) as shown in Figure 4. Specifically, the no-doped graphene-based antenna achieved a return loss of -28.2 dB, while WS_2 and $MoSe_2$ reached -14 dB and -10 dB, respectively.

4.2. Results and Discussion on the Graphene-Based Multilayer Antenna

The antenna illustrated in Figure 1 was designed and simulated using CST. To enable reconfigurability of both the bandwidth and the resonance frequency, different values of the chemical potential were applied: $\mu_c = 0$ eV, 0.2 eV, 0.3 eV, and 0.4 eV. A monolayer of graphene, matching the substrate surface and with a thickness of 0.01 µm, served as the active element. A broadband source was used to excite the structure, with a circular copper patch placed above the graphene layer thickness 0.15 µm. Figure 5 shows the simulated reflection coefficients

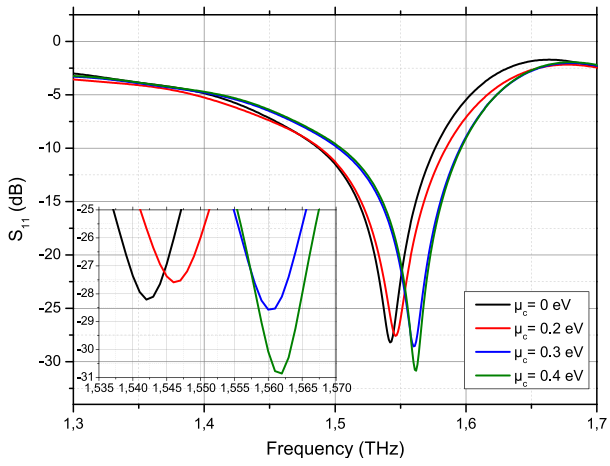

FIGURE 5. Reflection coefficient S_{11} for various chemical potential values.

for the four values of μ_c. The corresponding resonance frequencies were 1.542 THz, 1.547 THz, 1.560 THz, and 1.562 THz, respectively. The bandwidth varied between 91 and 96 GHz.

As shown in Figure 6, tuning the chemical potential effectively reconfigures the antenna's spectral characteristics. At $\mu_c = 0$ eV, the resonance occurs at $f_{r1} = 1.542$ THz, with a bandwidth of 91 GHz (1.487–1.578 THz). Increasing μ_c to 0.2 eV shifts the resonance to 1.547 THz, with a wider bandwidth of 94 GHz. At 0.3 eV and 0.4 eV, the resonance further shifts to 1.560 THz and 1.562 THz, respectively, with respective bandwidths of 92 GHz and 96 GHz. These shifts demonstrate an effective tuning mechanism for both bandwidth and resonance frequency. Moreover, the return loss improves from -28.2 dB at $\mu_c = 0$ eV to -30.8 dB at $\mu_c = 0.4$ eV, indicating enhanced impedance matching.

Table 2 confirms the observed spectral reconfigurability. The resonance frequency increases by about 1.36% from 1.541 to 1.562 THz, while the bandwidth enhances by nearly 5.5%. The best performance is obtained at $\mu_c = 0.4$ eV, showing the lowest return loss and widest bandwidth. Figure 7 and Figure 8 explore the influence of temperature and relaxation time on the antenna performance. As the temperature increases from 200 K to 400 K, the resonance frequency shifts from 1.540 THz to 1.548 THz, and the bandwidth grows from 89 GHz to 94 GHz. This indicates that temperature can be used as a secondary control variable for spectral tuning. For the relaxation time variation from 0.1 ps to 0.9 ps yields a resonance shift from 1.542 THz to 1.548 THz and a bandwidth increase from 91 to 95 GHz. This highlights the strong dependence of antenna performance on carrier scattering dynamics in graphene. These findings demonstrate that multiple parameters chemical potential, temperature, and relaxation time can be employed to finely tune the electromagnetic response of the proposed graphene-based THz antenna. The resonance frequency can be adjusted by approximately 0.52% through temperature variation and 0.39% through relaxation time tuning, while chemical potential modulation achieves the largest shift, up to 1.36%. Regarding bandwidth, temperature and relaxation time lead to increases of about 5.62% and 4.40%, respectively, whereas chem-

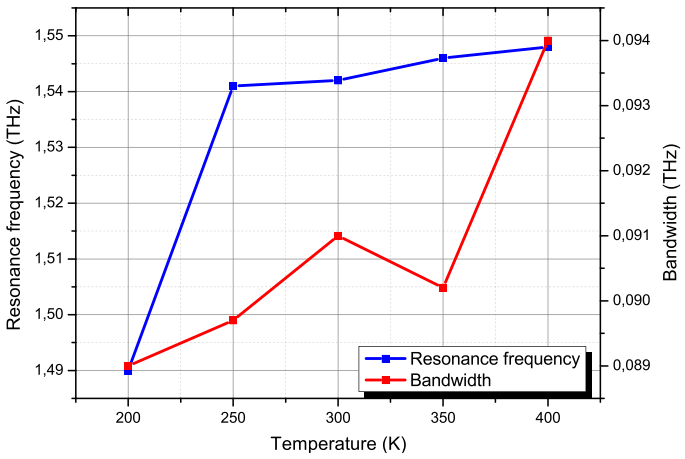

FIGURE 7. Impact of temperature on resonance frequency and bandwidth.

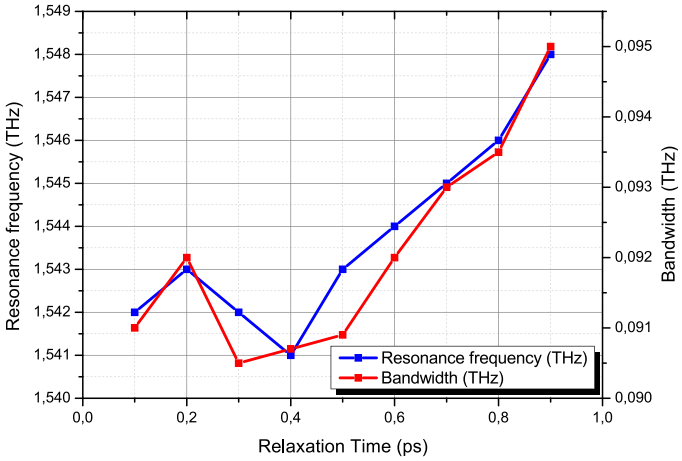

FIGURE 8. Impact of relaxation time on resonance frequency and bandwidth.

TABLE 2. Performance of the proposed antenna for various chemical potential values.

Chemical Potential (μ_c)	Resonant Frequency f_r (THz)	Bandwidth (GHz)	Reflection Coefficient S_{11} (dB)
0.0 eV	1.542	91	−28.2
0.2 eV	1.547	94	−27.5
0.3 eV	1.560	92	−28.5
0.4 eV	1.562	96	−30.8

TABLE 3. Comparative performance analysis of graphene based THz antennas.

Ref.	Resonance frequency (THz)	Bandwidth (GHz)	Return Loss (dB)	Feature
[29]	5.825	110	−44	Patch array on photonic crystal substrate
[30]	0.263	< 90 (narrow)	−33	Hybrid on-chip graphene patch
This work	1.562	96	−30.8	Hybrid Copper-Graphene multilayer

ical potential tuning provides the highest enhancement, up to 5.49%. These results confirm that chemical potential is the most effective parameter for achieving significant reconfiguration in both resonance frequency and bandwidth. Table 3 summarizes a comparative analysis of representative graphene-based THz antennas. The design in [29] achieves a resonance frequency around 5.8 THz with a bandwidth of 110 GHz and a return loss of −44 dB, whereas the integrated on-chip patch in [30] provides a tunability of about 38 GHz but remains narrowband (< 90 GHz) with a return loss of about −33 dB. In contrast, our hybrid Copper-graphene multilayer antenna operates at 1.562 THz with a bandwidth of 96 GHz and a return loss of −30.8 dB, which is comparable to or better than prior works in terms of wideband performance while keeping a competitive impedance matching. More importantly, unlike previous studies that rely exclusively on full wave electromagnetic simulations, our approach incorporates machine learning prediction of resonance frequency and bandwidth. This predictive capability enables accurate performance estimation with fewer simulations, significantly reducing computational cost and highlighting the novelty of the proposed methodology. To accelerate the structure design workflow, we integrate electromagnetic simulations with machine learning algorithms that predict key performance metrics such as resonance frequency and bandwidth. Traditional approaches, such as exhaustive full-wave sweeps, typically require over 30 hours for 300 configurations due to high mesh resolution and iterative solver convergence [31]. In contrast, our trained machine learning (ML) models (Random Forest, XGBoost) offer near-instantaneous predictions, significantly reducing design time. Despite their speed, these models maintain strong agreement with simulated data. This hybrid strategy, combining physics based modeling with data-driven learning, ensures both efficiency and reliability. Similar ML-driven accelerations have gained traction in recent metasurface optimization studies [32]. The following section presents the implementation and performance of our ML based framework.

5. PREDICTION OF RESONANT FREQUENCY AND BANDWIDTH

Machine learning models were employed to support the reconfigurability analysis by predicting the resonant frequency and bandwidth from the key parameters (chemical potential, tem-

TABLE 4. Performance comparison of Random Forest and XGBoost models for f_r and BW prediction.

Model	Target	MSE	RMSE	R^2
Random Forest	Resonant Frequency	2.13×10^{-6}	0.00146	0.9924
Random Forest	Bandwidth	4.37×10^{-7}	0.00066	0.9952
XGBoost	Resonant Frequency	1.26×10^{-6}	0.00112	0.9955
XGBoost	Bandwidth	4.48×10^{-7}	0.00067	0.9951

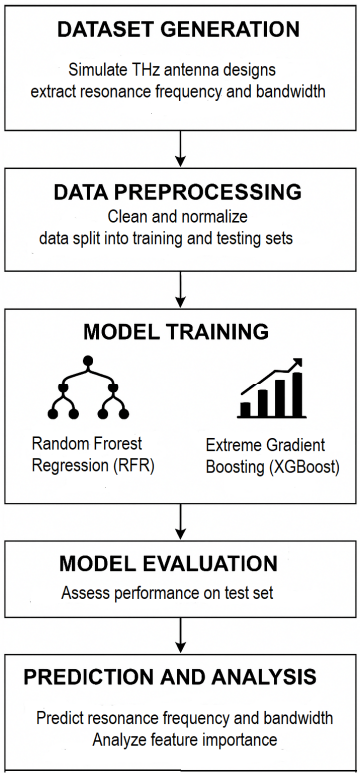

FIGURE 9. Overview of the proposed machine learning-based approach for THz antenna prediction.

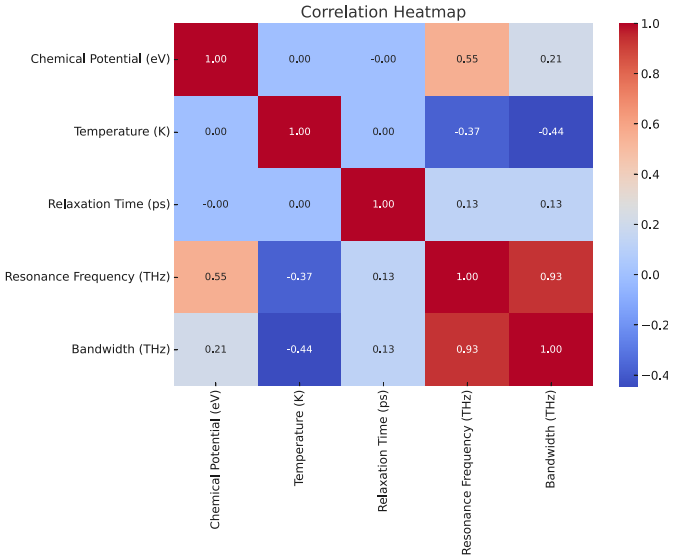

FIGURE 10. Correlation heatmap between input parameters and target values (f_r, BW).

perature, and relaxation time). A dataset of 300 CST simulations was generated and randomly split into 80% for training and 20% for testing. Performance was evaluated using standard regression metrics (mean square error (MSE), root mean square error (RMSE), and R^2). Two ensemble methods were implemented: Random Forest (200 estimators, depth $=$ 10) and XGBoost (300 estimators, depth $=$ 6, learning rate $=$ 0.1), with five-fold cross-validation to ensure robustness. Random Forest offers efficiency and stability by averaging multiple parallel decision trees, while XGBoost achieves higher accuracy through sequential gradient-based optimization, albeit at higher computational cost. These algorithms were chosen over deep learning, which typically requires much larger datasets. Both models achieved excellent accuracy ($R^2 > 0.99$), confirming strong agreement with CST simulations and demonstrating their suitability for fast and reliable antenna performance prediction. Figure 9 presents the overall workflow of the proposed ML-based method for predicting the resonance frequency and bandwidth of the THz graphene based antenna. The dataset is generated from simulations, preprocessed (normalization, correlation, train/test split), and used to train Random Forest and XGBoost models with cross-validation. Model performance is assessed by RMSE and R^2, while feature importance highlights the influence of physical parameters (μ_c, T, τ) on device behavior. Figure 10 shows that the chemical potential has the strongest correlation with the resonant frequency (0.55) and the highest positive link to the bandwidth (0.21). Temperature exhibits a moderate negative correlation with both outputs, while the relaxation time has only a weak influence (0.13). These results confirm that μ_c is the key parameter for jointly optimizing f_r and bandwidth (BW). Two regression models were implemented and evaluated: Random Forest (RF) and eXtreme Gradient Boosting (XGBoost). The dataset was randomly split into 80% for training and 20% for testing. The performance of each model was assessed using standard regression metrics, including MSE, RMSE, and the coefficient of determination (R^2), as summarized in Table 4.

Figures 11 and 12 show the predicted versus actual values for resonant frequency and bandwidth, respectively, obtained from the Random Forest (RF) model. Similarly, Figures 13 and 14 present the predicted versus actual values for resonant frequency and bandwidth, respectively, obtained from the XGBoost model. A strong agreement is observed in both cases, with XGBoost exhibiting slightly better generalization performance. These results confirm that machine learning models can accurately predict the antenna's performance metrics, thereby enabling efficient design space exploration. The strong influ-

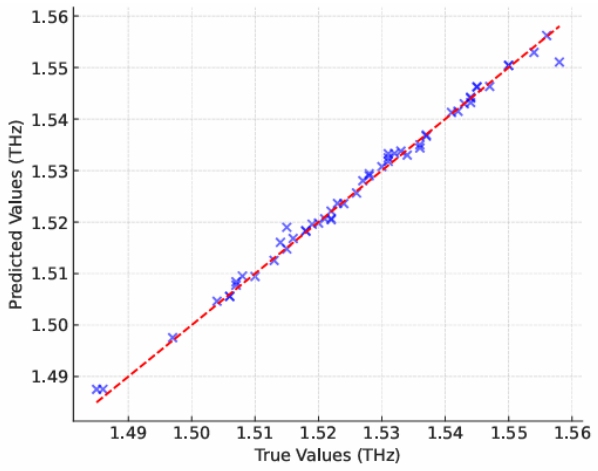

FIGURE 11. Correlation between predicted and true resonance frequency values using the Random Forest model.

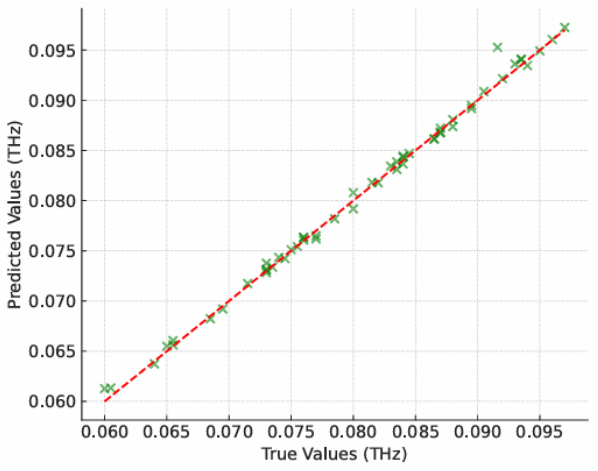

FIGURE 12. Correlation between predicted and true bandwidth values using the Random Forest model.

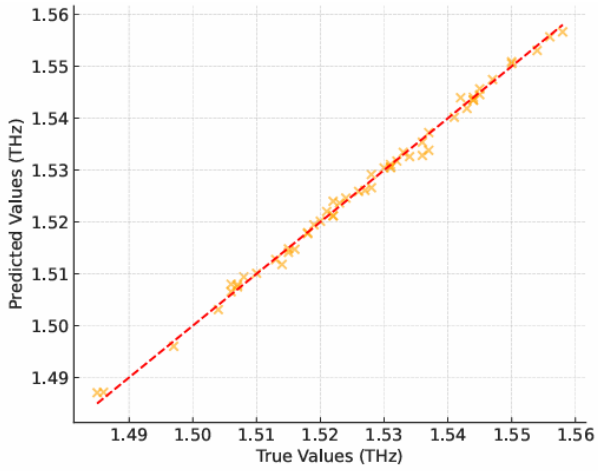

FIGURE 13. Correlation between predicted and true resonance frequency values using the XGBoost model.

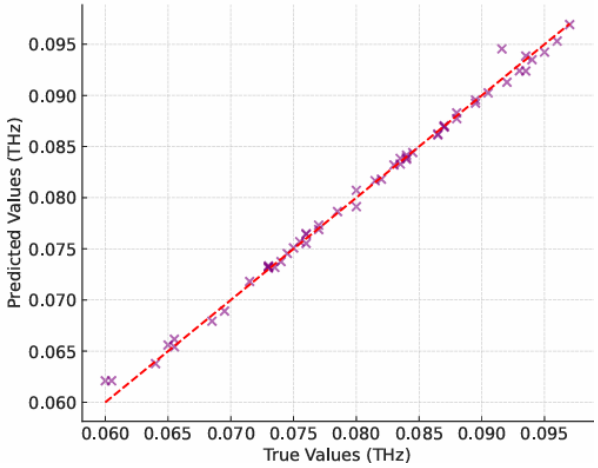

FIGURE 14. Correlation between predicted and true bandwidth values using XGBoost model.

ence of the chemical potential on the resonant frequency further highlights the high tunability potential of graphene in terahertz applications.

6. CONCLUSION

In this work, we present a reconfigurable multilayer graphene-based antenna for terahertz sensing, supported by machine learning-assisted estimation of resonance frequency and bandwidth. Compared to other two-dimensional materials such as Al_2O_3 and SiO_2, graphene demonstrated superior electromagnetic tunability. The proposed antenna achieved a resonance shift from 1.542 to 1.562 THz (a 96 GHz range), which represents a remarkable variation at terahertz scales. This reconfigurability enables selective sensing, dynamic operation, and enhanced adaptability of future wireless systems. Improvements in bandwidth and return loss were also observed. The correctness of the presented results was ensured through CST full-wave simulations consistent with the Kubo conductivity model of graphene. Machine learning models (Random Forest and XGBoost) trained on the generated dataset achieved $R^2 > 0.99$, showing excellent agreement with CST predictions. These findings, in line with recent studies [33–35], confirm the reliability of the proposed approach and highlight its potential for future terahertz applications. It should be emphasized that this study is based on full-wave CST simulations combined with ML-assisted predictions. While this approach provides valuable insights into the reconfigurability of the proposed antenna, experimental validation through prototype fabrication and measurements remains as future work. The practical implementation at terahertz frequencies is challenging due to graphene fabrication, multilayer integration, and biasing circuitry for chemical potential tuning. Addressing these challenges will be the focus of future research.

REFERENCES

[1] O'Hara, J. F., S. Ekin, W. Choi, and I. Song, "A perspective on terahertz next-generation wireless communications," *Technologies*, Vol. 7, No. 2, 43, 2019.

[2] Chaccour, C., M. N. Soorki, W. Saad, M. Bennis, P. Popovski, and M. Debbah, "Seven defining features of terahertz (THz) wireless systems: A fellowship of communication and sensing," *IEEE Communications Surveys & Tutorials*, Vol. 24, No. 2, 967–993, 2022.

[3] De Maagt, P., R. Gonzalo, Y. C. Vardaxoglou, and J.-M. Baracco, "Electromagnetic bandgap antennas and components for microwave and (sub)millimeter wave applications," *IEEE Transactions on Antennas and Propagation*, Vol. 51, No. 10, 2667–2677, 2003.

[4] Jamshed, M. A., A. Nauman, M. A. B. Abbasi, and S. W. Kim, "Antenna selection and designing for THz applications: Suitability and performance evaluation: A survey," *IEEE Access*, Vol. 8, 113 246–113 261, 2020.

[5] Thomas, S., J. S. Virdi, A. Babakhani, and I. P. Roberts, "A survey on advancements in THz technology for 6G: Systems, circuits, antennas, and experiments," *IEEE Open Journal of The Communications Society*, Vol. 6, 1998–2016, 2025.

[6] Anitha, V., A. Beohar, and A. Nella, "THz imaging technology trends and wide variety of applications: A detailed survey," *Plasmonics*, Vol. 18, No. 2, 441–483, 2023.

[7] Ullah, Z., G. Witjaksono, I. Nawi, N. Tansu, M. I. Khattak, and M. Junaid, "A review on the development of tunable graphene nanoantennas for terahertz optoelectronic and plasmonic applications," *Sensors*, Vol. 20, No. 5, 1401, 2020.

[8] Sharma, K., A. Karmakar, M. Sharma, A. Chauhan, S. Bansal, M. Hooda, S. Kumar, N. Gupta, and A. K. Singh, "Reconfigurable dual notch band antenna on Si-substrate integrated with RF MEMS SP4T switch for GPS, 3G, 4G, bluetooth, UWB and close range radar applications," *AEU — International Journal of Electronics and Communications*, Vol. 110, 152873, 2019.

[9] Taleb, R. D., M. Z. Baba-Ahmed, and M. A. Rabah, "Reconfigurable graphene antenna for a network cognitive radio: A novel solution for X-band satellite communications," *Advances in Space Research*, Vol. 73, No. 9, 4742–4750, 2024.

[10] Riaz, A., S. Khan, and T. Arslan, "Design and modelling of graphene-based flexible 5G antenna for next-generation wearable head imaging systems," *Micromachines*, Vol. 14, No. 3, 610, 2023.

[11] Hillger, P., J. Grzyb, R. Jain, and U. R. Pfeiffer, "Terahertz imaging and sensing applications with silicon-based technologies," *IEEE Transactions on Terahertz Science and Technology*, Vol. 9, No. 1, 1–19, 2019.

[12] Gupta, A., V. Kumar, S. Bansal, M. H. Alsharif, A. Jahid, and H.-S. Cho, "A miniaturized tri-band implantable antenna for ISM/WMTS/lower UWB/Wi-Fi frequencies," *Sensors*, Vol. 23, No. 15, 6989, 2023.

[13] Ahmad, I., W. Tan, Q. Ali, and H. Sun, "Latest performance improvement strategies and techniques used in 5G antenna designing technology, a comprehensive study," *Micromachines*, Vol. 13, No. 5, 717, 2022.

[14] Alibakhshikenari, M., E. M. Ali, M. Soruri, M. Dalarsson, M. Naser-Moghadasi, B. S. Virdee, C. Stefanovic, A. Pietrenko-Dabrowska, S. Koziel, S. Szczepanski, and E. Limiti, "A comprehensive survey on antennas on-chip based on metamaterial, metasurface, and substrate integrated waveguide principles for millimeter-waves and terahertz integrated circuits and systems," *IEEE Access*, Vol. 10, 3668–3692, 2022.

[15] Elalaouy, O., M. E. Ghzaoui, and J. Foshi, "THz antennas: Applications and challenges — A review," *Next Generation Wireless Communication: Advances in Optical, mm-Wave, and THz Technologies*, 235–249, 2024.

[16] Xu, M., T. Liang, M. Shi, and H. Chen, "Graphene-like two-dimensional materials," *Chemical Reviews*, Vol. 113, No. 5, 3766–3798, 2013.

[17] Jana, S., A. Bandyopadhyay, S. Datta, D. Bhattacharya, and D. Jana, "Emerging properties of carbon based 2D material beyond graphene," *Journal of Physics: Condensed Matter*, Vol. 34, No. 5, 053001, 2021.

[18] Preety, N. H., "Broadband, polarization insensitive and tunable THz metamaterial absorber using graphene and phase change material," Ph.D. dissertation, BRAC University, Dhaka, Bangladesh, 2024.

[19] Nicole, L., C. Laberty-Robert, L. Rozes, and C. Sanchez, "Hybrid materials science: A promised land for the integrative design of multifunctional materials," *Nanoscale*, Vol. 6, No. 12, 6267–6292, 2014.

[20] Chaparala, R., S. Imamvali, S. Tupakula, K. Prakash, S. Bansal, M. M. Ismail, and A. J. A. Al-Gburi, "Spoof surface plasmon polaritons-based feeder for a dielectric rod antenna at microwave frequencies," *Progress In Electromagnetics Research M*, Vol. 129, 23–32, 2024.

[21] Tishchenko, A., M. Khalily, A. Shojaeifard, F. Burton, E. Björnson, M. D. Renzo, and R. Tafazolli, "The emergence of multifunctional and hybrid reconfigurable intelligent surfaces for integrated sensing and communications — A survey," *IEEE Communications Surveys & Tutorials*, 2025.

[22] Haque, M. A., R. A. Ananta, J. H. Nirob, M. S. Ahammed, N. S. S. Singh, L. C. Paul, A. D. Algarni, M. ElAffendi, and A. A. Ateya, "Performance improvement of THz MIMO antenna with graphene and prediction bandwidth through machine learning analysis for 6G application," *Results in Engineering*, Vol. 24, 103216, 2024.

[23] Wekalao, J., H. A. Elsayed, A. M. El-Sherbeeny, M. R. Abukhadra, and A. Mehaney, "Design and optimization of a graphene-enhanced terahertz metasurfaces surface plasmon resonance biosensor with multi-material architecture for cancer detection integrating 1D-CNN machine learning for performance prediction and analysis," *Plasmonics*, 1–23, 2025.

[24] Yu, M., J. Yan, J. Chu, H. Qi, P. Xu, S. Liu, L. Zhou, and J. Gao, "Accurate prediction of wood moisture content using terahertz time-domain spectroscopy combined with machine learning algorithms," *Industrial Crops and Products*, Vol. 227, 120771, 2025.

[25] Ben Krid, H., Z. Houaneb, and H. Zairi, "Reconfigurable graphene annular ring antenna for medical and imaging applications," *Progress In Electromagnetics Research M*, Vol. 89, 53–62, 2020.

[26] Ben Krid, H., Z. Houaneb, and H. Zairi, "Reconfigurable hybrid metal-graphene UWB filters for terahertz applications," *Progress In Electromagnetics Research C*, Vol. 125, 241–251, 2022.

[27] Hlali, A., Z. Houaneb, and H. Zairi, "Non-reciprocal antenna array based on magnetized graphene for THz applications using the iterative method," *Progress In Electromagnetics Research M*, Vol. 89, 93–100, 2020.

[28] Hlali, A., Z. Houaneb, and H. Zairi, "Dual-band reconfigurable graphene-based patch antenna in terahertz band: Design, analysis and modeling using WCIP method," *Progress In Electromagnetics Research C*, Vol. 87, 213–226, 2018.

[29] Kumar, C., S. K. Raghuwanshi, and V. Kumar, "Graphene-based patch antenna array on photonic crystal substrate at terahertz frequency band," *Journal of Electromagnetic Waves and Applications*, Vol. 38, No. 2, 250–263, 2024.

[30] De Santana, E. P., A. K. Wigger, Z. Wang, K.-T. Wang, M. Lemme, S. Abadal, and P. H. Bolívar, "Integrated graphene patch antenna for communications at THz frequencies," in *2022 47th International Conference on Infrared, Millimeter and Terahertz Waves (IRMMW-THz)*, 1–2, Delft, Netherlands, 2022.

[31] Rebeiz, G. M., *Millimeter-Wave Antennas and Arrays*, John Wiley & Sons, 2007.

[32] Lin, H., J. Hou, J. Jin, Y. Wang, R. Tang, X. Shi, Y. Tian, and W. Xu, "Machine-learning-assisted inverse design of scattering enhanced metasurface," *Optics Express*, Vol. 30, No. 2, 3076–3088, 2022.

[33] Gezimati, M. and G. Singh, "Terahertz imaging and sensing for healthcare: Current status and future perspectives," *IEEE Access*, Vol. 11, 18 590–18 619, 2023.

[34] Gezimati, M. and G. Singh, "Terahertz data extraction and analysis based on deep learning techniques for emerging applications," *IEEE Access*, Vol. 12, 21 174–21 198, 2024.

[35] Malhotra, I. and G. Singh, *Terahertz Antenna Technology for Imaging and Sensing Applications*, Springer, Cham, Switzerland, 2021.